

Accepted Manuscript

Effects of splice joint geometry and bolt torque on the serviceability response of pultruded glass fibre reinforced polymer composite beams

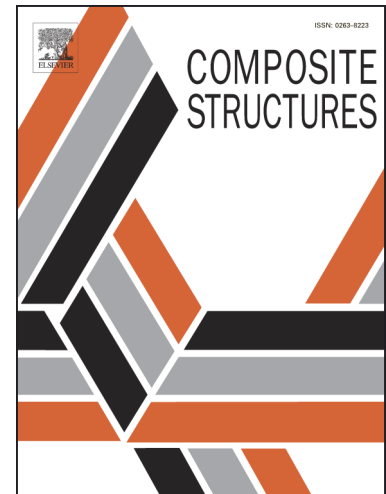
G.J. Turvey, X. Cerutti

PII: S0263-8223(15)00395-5

DOI: <http://dx.doi.org/10.1016/j.compstruct.2015.05.030>

Reference: COST 6448

To appear in: *Composite Structures*



Please cite this article as: Turvey, G.J., Cerutti, X., Effects of splice joint geometry and bolt torque on the serviceability response of pultruded glass fibre reinforced polymer composite beams, *Composite Structures* (2015), doi: <http://dx.doi.org/10.1016/j.compstruct.2015.05.030>

This is a PDF file of an unedited manuscript that has been accepted for publication. As a service to our customers we are providing this early version of the manuscript. The manuscript will undergo copyediting, typesetting, and review of the resulting proof before it is published in its final form. Please note that during the production process errors may be discovered which could affect the content, and all legal disclaimers that apply to the journal pertain.

Effects of splice joint geometry and bolt torque on the serviceability response of pultruded glass fibre reinforced polymer composite beams

by

G.J. Turvey^{a,*} and X. Cerutti^{a,b,*}

^a Engineering Department, Lancaster University, Bailrigg, Lancaster, LA1 4YR, UK

(Corresponding author: Tel.: +44(0)1524 593088; g.turvey@lancaster.ac.uk)

^b Centre for Material Forming – CEMEF, CNRS UMR 7635, 1 rue Claude Daunesse, 06904 Sophia-Antipolis, France

Keywords: Beams, Bolts, GFRP, Pultrusion, Splice Joints

Abstract

Thirty-six, four-point flexure tests on simply supported pultruded glass fibre reinforced polymer composite (GFRP) Wide Flange (WF) beams with mid-span bolted splice joints are described. The joints were fabricated with two and six pultruded GFRP splice plates. Three splice plate lengths were investigated and two bolt torques were used to tighten the bolts. Each of the twelve splice joint combinations was subjected to three repeat tests up to the serviceability deflection limit. Their load versus deformation responses were shown to be linear and repeatable. During each test loads, support rotations, splice joint end rotations and mid-span surface strains were recorded for each mid-span deflection increment. The beams' transverse stiffnesses and splice joints' rotational stiffnesses were derived from the test data. The variation of the stiffnesses with splice plate length, number of splice plates and bolt torque was also quantified. A simple analysis was developed for splice-jointed beams and was used to predict the transverse and rotational stiffnesses determined from the test data. It was shown that the transverse stiffnesses could be predicted to within 10%, provided a rigid-body rotational correction was applied. The correction also provided an estimate of the splice joint's slip displacement.

1. Introduction

During the course of the past three decades a considerable volume of research literature has accumulated on the behaviour of bolted joints used in structures fabricated from pultruded glass fibre reinforced polymer (GFRP) composite components such as flat plate and open/closed section profiles. Most of the research literature may be sub-divided into two groups, namely bolted plate-to-plate tension joints and bolted flexural joints in frame structures. A summary of much of the early literature on the former group may be found in [1], and the more recent literature is reviewed in [2] and [3]. Likewise, much of the early literature on the second group is reviewed in [4] and a more up-to-date review may be found in [5]. Much of this research has contributed to the development of design guidance for these two groups of joints (see, for example, [6] – [8]).

In sharp contrast to the aforementioned relatively extensive research literature on mechanically fastened tension and beam-to-column joints, research on both bonded and bolted splice joints is, to say the least, limited. Such joints are used to create end-to-end continuity between beam profiles via splice plates which may be mechanically fastened and/or adhesively bonded to their flanges and/or webs. In [9] flexural tests were reported on equal, two-span box-section beams in which continuity was provided by adhesively bonded pultruded GFRP plates at the interior support. The principal objective of that investigation was to demonstrate that pseudo-ductility could be achieved during failure of the continuous beam by using a ductile adhesive within the splice joint. Somewhat later, experimental and analytical research on the flexural behaviour of single-span simply supported GFRP beams with pultruded GFRP bonded splice joints at mid-span was reported in [10] and [11]. In addition to quantifying the effect of the splice joints on the beams' transverse stiffnesses, the rotations recorded at the extremities of the splice joints in [10] enabled their rotational stiffnesses to be quantified. The analytical developments presented in [11] quantified optimal splice plate lengths and compared the relative effects of splice plate materials (GFRP versus CFRP) and their geometries on the transverse stiffnesses of such beams.

Tests on simply supported single-span pultruded GFRP box- and WF-section beams with bolted splice joints at mid-span were reported in [12] and [13]. Although the focus of the latter research was predominantly on the fatigue behaviour of the beams, a few three-point static flexure tests were reported. The simply supported beams were 102 mm deep with 6.35 mm web and flange thicknesses. Their spans were 1.83 m and the thickness of the

splice plates were twice that of the web(s) and flanges of the beam sections. 9.5 mm diameter bolts, torqued to 27.1 Nm, were used in the splice joints. An interesting feature was the unsymmetric staggered bolt layout used in the web splice plates; the reason(s) for adopting this bolt layout were not explained. A more recent investigation of single-span simply supported pultruded hybrid-fibre beams (GFRP webs and GFRP/CFRP flanges) with mid-span splice joints was reported in [14]. The 250 mm deep beams were tested to failure in four-point flexure with spans of 3 m. The steel splice plates were bolted and bonded to the beams' web and flanges using two layouts of 10 mm diameter bolts. A novel feature was the serrated inner faces of the splice plates to enhance the strength of the adhesive bond in the bolted and bonded splice joints. The authors modelled their tests using a three-dimensional, nonlinear ABAQUS [15] FE analysis and were able, for the most part, to demonstrate good agreement with their test results. In [16] a series of three-point flexure tests were reported on single-span, simply supported, pultruded GFRP beams with bolted pultruded GFRP splice joints of fixed length at mid-span. The primary focus of the test work was to explore the effect of increasing bolt torque on the beams' serviceability responses with respect to their major and minor planes of flexure.

The present paper develops the experimental investigation reported in [16] by changing the loading arrangement to four-point bending, so that the rotational stiffnesses of the splice joints may also be quantified. In addition, different splice plate lengths are considered in order to explore their effect on serviceability deformations. Furthermore, the test work is complemented by the development of an analysis for predicting the mid-span deflections of bolted splice-jointed pultruded GFRP beams.

The structure of the paper takes the following form. First, the material properties of the pultruded GFRP beams and splice plates are presented. This is followed by descriptions of the splice joint layouts and the overall geometry of the splice-jointed beams. Details of the bolts and the bolt torques are then given. Thereafter, a description of the test setup, instrumentation and loading procedure follows. Sample results, which illustrate the repeatability/consistency of the test results, are presented. Then the main sets of test results, which quantify the effects of bolt torque, splice plate length and number of splice plates on the beams' transverse stiffnesses and the splice joints' rotational stiffnesses, are presented. An analytical procedure, based on the Method of Transformed Sections and Mohr's Theorems [17] for determining the mid-span deflections (and by implication the beams' transverse stiffnesses) of the spliced beams is explained and comparisons of the predicted and experimental deflections are presented. Finally, the main conclusions of the investigation are summarised.

2. Longitudinal elastic moduli of the pultruded GFRP beams and splice plates

152 x 152 x 6.4 mm (nominal dimensions) pultruded GFRP wide-flange (WF) beams were used in all of the spliced beam tests. Likewise, 6.4 mm thick pultruded GFRP flat plates were used in all of the splice joints. In both types of profile the fibre reinforcement was alternate layers of E-glass rovings and continuous filament mat (CFM), and the matrix material was a mixture of unsaturated polyester resin and filler (typically kaolin). In the WF profiles the rovings were in contact transverse to the pultrusion direction and in the plate profiles they were several millimetres apart in that direction. In consequence, the fibre volume percentage of the splice plates was lower than that of the beams and, therefore, their longitudinal elastic modulus was expected to be lower.

A number of tension coupon tests were carried out on rectangular coupons cut out of the web and flanges of the WF beam and the flat plate to determine their longitudinal elastic moduli. The average values of the longitudinal elastic moduli, determined from the coupon tests, confirmed that the beam profiles had the higher modulus. In Table 1 the average values of the beam and plate moduli are compared with the manufacturer's corresponding minimum values [18]. It is evident that the beam's elastic modulus is nearly 14% greater than the plate's modulus and, moreover, the manufacturer's minimum moduli are only 84% and 69% of the beam and plate average moduli, respectively.

3. Bolted splice plate details

In this investigation, the differences between the splice joints are defined in terms of the number and length of the splice plates and the bolt torques. Three splice plate lengths were used, namely 210 mm, 410 mm and 610 mm. Hence, the splice plate length to beam depth ratio ranged from 1.38 to 4.01. Furthermore, the span of the splice-jointed beams was 2.9 m, so that the splice plate length to span ratio ranged from 0.072 to 0.210. The splice plates bolted to the outer surfaces of the beams' flanges had the same width as the flanges and their length to width ratios were identical to their length to beam depth ratios. However, the splice plates bolted to the inner surfaces of the beams' flanges were only 68 mm wide, so that their length to width ratios ranged from 3.09 to 8.97.

10 mm diameter stainless steel bolts were used to fasten the splice plates to the flanges of the pultruded GFRP beams. Web splice plates were not used. The bolt shanks were smooth and sufficiently long, so that there was no thread contact with the cylindrical surface of the bolt holes. The diameter of the smooth bolt shank was typically 0.2 mm smaller than the bolt's nominal diameter. Therefore, even though the nominal diameters of the bolts and bolt holes were identical, small hole clearances were unavoidable. One standard size washer (23 mm x 10.5 mm x 2 mm) was used under each bolt head and nut. Furthermore, a calibrated torque wrench was used to tighten the bolts to 3 Nm (finger-tight) or 20 Nm.

Figure 1(a) shows half of a 610 x 152 x 6.4 mm outer splice plate with two columns of 10 mm diameter bolt holes and Figure 1 (b) shows half of a 610 x 68 x 6.4 mm inner splice plate with one column of 10 mm diameter bolt holes. The centre-to-centre distance between the bolt holes is 100 mm, except for the innermost pair of holes, for which the distance is 110 mm to accommodate the 10 mm gap between the beam ends within the splice joint. The half lengths of the 410 mm and 210 mm splice plates may be envisaged by shortening the diagrams in Figures 1(a) and (b) in turn by 100 mm and 200 mm and deleting the corresponding row(s) of bolt holes.

4. Splice joint layouts and fabrication details

Figures 2(a), 2(b) and 2(c) show side elevations of 610 mm, 410 mm and 210 mm long six-plate bolted splice joints at the mid-spans of pultruded GFRP beams and Figure 2(d) shows their end elevations. The corresponding two-plate bolted splice joints may be envisaged by removing the splice plates from the inner surfaces of the top and bottom flanges in Figures 2(a) – 2(c) and the splice plates from the inner surfaces of the top and bottom flanges in Figure 2(d).

In order to simplify the fabrication of the splice joints and to minimise positioning errors of the bolt holes in the splice plates, it was deemed sensible to use templates. Hence, twelve bolt holes were drilled in one of the 610 mm outer splice plates (see Figure 1(a)). This template splice plate was then clamped to outer surface of the flanges of the two half-beams with a 10 mm gap between their ends and two narrower 610 mm splice plates (see Figure 1(b)) were clamped to the inner surfaces of the flange on each side of the web. Then, using the outer template splice plate as a guide, twelve bolt holes were drilled through the flange and the inner splice plates. Twelve 10 mm diameter bolts were then inserted into the holes and torqued to 3 Nm. The process was then repeated for the other flanges of the two half-beams to complete the fabrication of the 610 mm six-plate splice joint. A similar fabrication procedure was used to fabricate the 410 mm and 210 mm long six-plate splice joints. Two-plate splice joints for each of the three lengths were obtained by undoing the bolts, removing the four inner splice plates, and then tightening the bolts to the required torque.

5. Splice beam test setup, instrumentation, loading procedure and test matrix

As mentioned in the Introduction, a four-point flexural test configuration with the loading points outside of the ends of the splice joints was adopted, so that the transverse stiffnesses of the beams and the rotational stiffnesses of the splice joints could be determined for their serviceability limit deflections. The test configuration is shown in Figure 3. A dial gauge with a displacement resolution of 0.01 mm in contact with the centre of the lower outer splice plate at the mid-span position C was used to measure the deflections. Four clinometers attached at the level of the centre line of the web over the supports A and B and in line with the ends of the splice plates at D and E recorded the rotations at these locations. For small angles of rotation (less than 5°) the clinometers' angular resolution was 0.001°. Four unidirectional strain gauges were bonded to the outer splice plates at mid-span to record their outer surface tensile and compressive strains. The sensitive axis of each gauge was parallel to the longitudinal axis of the spliced beam; the gauge lengths and resistances were 10 mm and 120 ohms, respectively. Figure 4 shows the positions of the gauges on the central cross-section of a beam with a six-plate splice joint. The two loads were applied to the splice-jointed beams using a manually operated 50 kN capacity hydraulic jack. One end of a 10 kN capacity load cell was attached to the ram of the jack and its other end was attached to a steel loading beam which transmitted the loads to the top flange of the pultruded GFRP beam via circular cross-section steel rods at its ends. An image of the test rig is shown in Figure 5.

The test procedure adopted was to increase the load gradually to produce 1 mm increments of deflection at mid-span. Immediately after each displacement increment, the load was noted together with the rotations and strains, recorded by the four clinometers and four strain gauges, respectively. When the mid-span deflection reached 15 mm loading was stopped and the beam was unloaded in 1 mm decrements with the load, rotations and strains recorded immediately after each decrement. This load – unload procedure was repeated three times for each of the twelve different splice-jointed beams.

Table 2 gives an overview of the test matrix adopted for this series of tests on pultruded GFRP beams with mid-span bolted splice joints.

6. Repeatability of the serviceability load – deformation responses

As explained in Section 5, each load – unload test was repeated three times for each splice joint layout and bolt torque. In general, the loading and unloading – deformation responses were almost identical for each of the splice-jointed beams tested. Consequently, only the load – deformation responses are presented here to illustrate their repeatability and consistency. Load versus mid-span deflections for three tests on two splice-jointed beams with 410 mm long splice plates are shown in Figure 6. One of the beams had a two-plate splice joint with the bolts torqued to 3 Nm, and the other beam had a six-plate splice joint with the bolts torqued to 20 Nm. Both sets of load versus deflection responses are linear up to the deflection serviceability limit of 15 mm. There is a small difference between the Test 1 and Test 2 results, presumably due to *bedding-in* effects, but the Test 2 and Test 3 results are essentially identical. Figure 7 shows the load versus rotation responses at the simple support labelled A (see Figure 3) and confirms their linearity and repeatability. However, as shown in Figure 8, the moment versus splice joint rotation response is only linear for the two-plate splice joint with its bolts torqued to 3 Nm. Nevertheless, for Tests 2 and 3 both responses are repeatable.

7. Effects of splice joint geometry and bolt torque on transverse and rotational stiffnesses

Straight lines have been fitted to the load versus mid-span deflection data plots of the thirty-six tests identified in Table 2. From the slopes of the lines, the transverse stiffnesses of the splice-jointed beams have been quantified, based on Test 3 and the average of Tests 1-3 data. The two sets of transverse stiffnesses are given in Table 3. The transverse stiffnesses for two-plate splice joints are shown plotted against splice plate length in Figure 9. It is evident that transverse stiffness increases as the length of the splice plates increases and increasing the bolt torque by a factor of about 6.7 does not produce a commensurate increase in transverse stiffness. Moreover, for the 3 Nm bolt torque the increase in transverse stiffness due to increasing the splice plate length from 210 mm to 410 mm is significantly greater than that by further increasing its length to 610 mm, i.e. 39-42% compared to 7-8%. However, for the 20 Nm bolt torque, the corresponding increases in transverse stiffness due to increasing the lengths of the splice plates from 210 mm to 410 mm and from 410 mm to 610 mm are 31-33% and 17-18% respectively.

A similar plot showing the effects of number of splice plates and bolt torques on the beams' transverse stiffness is shown in Figure 10. Perhaps the most striking feature is that the transverse stiffnesses of beams with two-plate splice joints and bolts torqued to 20 Nm are nearly equal to the transverse stiffnesses of beams with six-plate splice joints and bolts torqued to 3 Nm. Again, it is evident that increasing bolt torque and splice plate length in beams with six-plate splice joints also increases the transverse stiffness. For a bolt torque of 3 Nm the percentage increases in transverse stiffness due to increasing the splice plate length from 210 mm to 410 mm and from 410 mm to 610 mm are 25% and 13% respectively. The corresponding percentage increases for a bolt torque of 20 Nm are 22% and 15% respectively.

In Figure 11 the percentage increases in transverse stiffness due to increasing bolt torque alone, and bolt torque and the number of splice plates are presented as a function of splice plate length. The percentage increases have been computed relative to the transverse stiffnesses of two-plate splice-jointed beams with splice plates of equal lengths and bolts torqued to 3 Nm. It is evident that the largest percentage increases in transverse stiffness are for the 210 mm ($N = 6$, $T = 20$ Nm) and 610 mm ($T = 20$ Nm) long splice plates, respectively.

Moment versus splice joint rotation graphs have been plotted using Test 3 data obtained from the splice-jointed beam tests. Straight lines have been fitted to the data points to determine the rotational stiffnesses of the splice joints. In addition, secant stiffnesses have also been determined from the maximum load and deflection data points. Both sets of stiffnesses are given in Table 4. It is evident that there is very little difference between corresponding stiffnesses for the Test 3 data, despite the fact that Figure 8 shows some evidence of nonlinearity in the moment versus rotation response for the 410 mm long six-plate splice joint with its bolts torqued to 20 Nm.

In Figure 12 the effect of increasing the bolt torque from 3 Nm to 20 Nm on rotational stiffnesses (based on straight line fits to the test data) are shown for two-plate splice joints. The increases in stiffness are 53%, 42% and 65% for the 210mm, 410 mm and 610 mm long splice joints, respectively. The rotational stiffness obtained for all of the joints (again based on straight line fits to the test data) are shown in Figure 13. Unlike the

transverse stiffnesses of the beams, not all of the joints' rotational stiffnesses increase with increasing splice length. For the two-plate splice joint with its bolts torqued to 3 Nm, its rotational stiffness with 610 mm long splice plates is lower than with 410 mm long splice plates. For all of the other splice joints, their rotational stiffnesses increase as the number of splice plates, splice plate lengths and bolt torques increase. It is also evident that two-plate splice joints with 410 mm and 610 mm long splice plates and bolts torqued to 20 Nm have the same rotational stiffnesses as six-plate splice joints with equally long splice plates but with bolts torqued to 3 Nm.

The final set of test results in Figure 14 show the percentage increases in splice joint rotational stiffness for different splice plate lengths as the bolt torque and the number of splice plates increases. It is significant that increasing the bolt torque of a two-plate splice joint from 3 Nm to 20 Nm increases its rotational stiffness by between 42% and 65% depending on the splice plate length, whereas adding four extra splice plates increases its rotational stiffness by between 101% and 156% for the same increase in bolt torque.

8. Analytical predictions of transverse deflections and rotations of splice-jointed beams

In [10] and [11] the first author used the Method of Transformed Sections and Mohr's Theorems [17] to develop formulae for predicting the deformations of pultruded GFRP beams with bonded splice joints. He demonstrated that, in general, the formulae provided reasonably good predictions of the mid-span deflections and support rotations up to the serviceability deflection limit, though the rotational stiffnesses of the bonded splice joints were predicted with significantly lower accuracy. In the light of the foregoing, the authors have used this approach to predict the serviceability deformations of pultruded GFRP beams with bolted pultruded GFRP splice joints, the details of which are given in the following sections.

9. Method of transformed sections for bolted splice joints

The Method of Transformed Sections [17] is used to convert a multi-material cross-sectional shape into an equivalent single material cross-sectional shape. The choice of which material the other materials should be transformed to is arbitrary. Here the GFRP splice plates and the steel bolts are transformed to equivalent GFRP WF beam material. This is achieved by modifying the width of the splice plates and the equivalent widths of the bolts by the ratio of their elastic moduli to the WF beam's longitudinal elastic modulus. Therefore, the width of the splice plates reduces (see Table 1) and that of the bolts increases. As the bolts have circular cross-sections, these have been transformed to equivalent rectangular cross-sections, i.e 7.58 mm x 10 mm. Sketches of the original and transformed cross-sections of a six-plate bolted splice joint are shown in Figures 15(a) and 15(b), respectively. The transformed section for a two-plate splice joint may be envisaged by removing the inner splice plates and reducing the depth of the bolts' transformed cross-section by the thickness of the inner splice plate.

The transformed section enables the second moment of area of the multi-material cross-section to be calculated for use in conjunction with Mohr's Moment-Area Theorems [17]. It is convenient to set up the second moment of area expression for the transformed cross-section of the bolted splice joint, shown in Figure 15(b), in terms of the cross-section contributions of the WF beam, the transformed cross-sections of the outer and inner splice plates and the bolts, all with respect to the major flexural axis. These contributions (and the definitions of their second moment of area symbols) are given in Table 5. Hence, the transformed second moment of area I of the six-plate bolted splice joint cross-section, depicted in Figure 15(b), may be expressed as,

$$I = I_s + I_{wo} + I_{wi} + I_{b1} + I_{b2} + I_{b3} \quad (1)$$

and the transformed second moment of area of the splice joint cross-section between the bolts is,

$$I = I_s + I_{wo} + I_{wi} \quad (2)$$

Likewise, the transformed second moments of area of the corresponding cross-sections of a two-plate bolted splice joint are obtained by setting $I_{wi} = I_{b3} = 0$ in Equation (1) and $I_{wi} = 0$ in Equation (2), respectively.

10. Mohr's Moment-Area theorems

The first of Mohr's Moment-Area theorems enables the angle between the tangents at two points on the deflection curve of a loaded beam to be determined. The second theorem enables the length of the vertical line

drawn from the second tangent point to the point where the first tangent intersects the line to be determined. The theorems are used to calculate slopes/rotations and deflections of beams. Further details of the application of the theorems are given in [17].

In order to apply Mohr's theorems to the pultruded GFRP splice jointed beam shown in Figure 3, it is necessary first to set up the bending moment diagram and then scale it by dividing by the product of the elastic modulus and the second moment of area, i.e. create what is commonly referred to as an $\frac{M}{EI}$ -diagram (where M is the bending moment and E is the longitudinal elastic modulus of the WF beam). The bolted splice-jointed beams considered here have a vertical axis of symmetry at mid-span. Therefore, it is only necessary to set up the $\frac{M}{EI}$ -diagram for half of the beam. However, because the beam is non-uniform along its length the resulting $\frac{M}{EI}$ -diagram is also non-uniform. The $\frac{M}{EI}$ -diagram for a pultruded GFRP beam with a 610 mm long bolted splice joint at mid-span is shown in Figure 16. Nine separate areas, A_i ($i = 1 - 9$), are identified corresponding to the unspliced, spliced and bolted spliced zones of the half-span. The equations for each area are given in Table 6 and the rotation at the support B (see Figure 3) is given as,

$$\theta_B = \sum_{i=1}^{i=9} A_i \quad (3)$$

In order to apply Mohr's second theorem to calculate the mid-span deflection, the distances G_i of the centres of the areas A_i ($i = 1 - 9$) from the support B must be determined. These distances are given in Table 7. Hence, using Mohr's second theorem, the mid-span deflection δ_C is given as,

$$\delta_C = \sum_{i=1}^{i=9} A_i G_i \quad (4)$$

The support rotations θ_B and the mid-span deflections δ_C for the pultruded GFRP beams with 210 mm and 410 mm long bolted splice joints at mid-span may be calculated using Equations (3) and (4) by setting up tables similar to Tables 6 and 7, but for corresponding reduced numbers of areas and centre of area distances.

The rotation at one end of the splice joint may be evaluated using the areas of the $\frac{M}{EI}$ -diagram which extend over the half-length of the splice joint, i.e. $A_3 - A_9$ (see Figure 16), in Equation (3). This rotation may then be used to estimate the rotational stiffness of the splice joint.

11. Comparison of analytical and experimental rotations and deflections

The formulae for A_i in Table 6 and G_i in Table 7 together with Equations (1) - (4) have been used to determine the values of θ_B and δ_C corresponding to the Test 3 maximum loads of the twelve tests on spliced jointed beams (see Table 2). It was found that the predicted support rotations and mid-span deflections significantly under-estimated the values recorded in the four-point bending tests (counting from the left, see the last column in Table 8 and columns 5 and 7 in Table 9). This outcome was not altogether surprising, despite the fact that the Method of Transformed Sections combined with Mohr's Moment-Area theorems had been shown to give reasonably accurate predictions for rotations and deflections of pultruded GFRP beams with mid-span bonded splice joints (see [10] and [11]).

On further reflection, it was felt that the presence of small clearances (of the order of 0.2 mm) in the bolt holes must have allowed relative movement (slip) to occur at the interfaces between the splice plates and the beam's

flanges. However, the analysis assumes full interaction (zero slip) between the flanges and splice plates and is, therefore, over-stiff. In order to improve the analysis's predictions, it was postulated that by applying the difference between the measured and predicted rotations at the support B as a rigid-body rotation to one half of the beam it might produce a meaningful deflection correction that could be added to the calculated mid-span deflection to produce a more accurate estimate of the experimental mid-span deflection (see Figure 17). Moreover, if the same rigid-body rotation was applied to the half-depth of the beam, it might also provide a meaningful estimate of half of the total slip between the flanges and the splice plates (see also Figure 17). Table 9 includes both the uncorrected and corrected mid-span deflections and compares them with the deflections recorded in the splice-jointed beam tests. In addition, the estimated slip displacement along each half of the splice joint is also given for each test. It is evident that the corrected mid-span deflections are, with two exceptions, always within 10% of the experimental values. Moreover, the slip displacements appear plausible given the 0.2 mm possible clearances between the bolt shanks and the cylindrical surfaces of the bolt holes. Even though reasonable estimates of the mid-span deflections of the splice jointed beams have been obtained by adding the deflection corrections derived from the rigid-body rotations of the half-beam illustrated in Figure 17, it must be appreciated that the magnitudes of these rotations are unknown *a priori*. Consequently, unless a method for determining the additional rigid-body rotation can be developed, the present approach cannot be used as a stand-alone method for predicting the mid-span deflections of splice-jointed pultruded GFRP beams.

The same approach was also used to predict the rotational stiffnesses of the bolted splice joints, but, unfortunately, it did not give reasonable predictions.

12. Concluding remarks

A total of thirty-six four point bending tests have been carried out on simply supported pultruded GFRP beams with bolted pultruded GFRP splice joints at their mid-spans. The splice-jointed beams were loaded up to the serviceability deformation limit. Repeat testing showed that, generally, the mid-span deflections, support rotations and splice joint rotations were consistently linear and repeatable.

The effects of three splice joint properties, namely the number of splice plates, their lengths and the bolt torque, on the transverse stiffnesses of the splice-jointed beams and the splice joint rotational stiffnesses were investigated in the tests. It was shown that the transverse stiffness of the two and six-plate splice-jointed beams increased as the splice plate lengths increased from 210mm to 610 mm. The transverse stiffnesses were, as expected, greater for the six-plate than the two-plate splice joints. Furthermore, it was shown that increasing the bolt torque from 3 Nm to 20 Nm increased the transverse stiffness, but not in proportion to the increase in bolt torque. It was also observed that, as the bolt torque and/or the number of splice plates increased, the transverse stiffness tended to increase linearly as the splice plate length increased. Percentage increases in transverse stiffness for two- and six-plate splice-jointed beams with 20 Nm bolt torques have been quantified relative to those of beams with two-plate splice joints and their bolts torqued to 3 Nm.

The effects of bolt torque and number of splice plates on the rotational stiffness of the splice joints as the length of the splice plates increased have been quantified. In addition, the percentage increases in the rotational stiffnesses of two- and six-plate joints with the higher bolt torque were also quantified relative the two-plate joint with bolts torqued to 3 Nm. As for the transverse stiffness, the greatest percentage increase in rotational stiffness was for the 210 mm long splice joint.

Details of the analysis of splice jointed beams using the Method of Transformed Sections and Mohr's two theorems have been presented. Equations for the contributions to the overall second moment of area of the transformed section of the splice joint have been given. In addition, the $\frac{M}{EI}$ -diagram for the right hand half of the spliced beam has been presented and equations for its component areas and the corresponding centre of area distances from the right hand support have also been given. In the final part of the analysis equations for the rotation at the right hand support and the mid-span deflection have been presented. These equations have been used to predict the support and splice joint rotations and mid-span deflection for the maximum load applied in third repeat test on each of the splice-jointed beams.

The predicted deformations have been compared with the corresponding measured deformations. It has been shown that both the support rotations and the mid-span deflections were significantly under-estimated, as also were the splice joint rotations. However, it has been demonstrated that by applying the difference between the predicted and the experimental support rotations as a rigid-body rotation to the half-span beam the resulting

mid-span deflection may be added to the under-estimated calculated deflection to give a more accurate estimate of the experimental deflection. This approach gave deflections generally within 10% of the measured values. The same rigid-body rotation applied to half of the beam's depth at mid-span also provided an estimate of the relative movement (slip) between the splice plate(s) and the flange for half of the splice joint. However, the accuracy or otherwise of this relative movement remains to be established.

Acknowledgements

The investigation reported herein was undertaken and completed in the Engineering Department's Structures Laboratory at Lancaster University. Both authors wish to express their appreciation for the help and assistance provided by the Engineering Department's technicians, without which the test work could not have been completed successfully.

References

1. Turvey GJ. Plate-to-plate mechanical: part II. Testing and applications. In *Semi-rigid behaviour of civil engineering structural connections, COST C1: State-of-the-art review on design, testing, analysis and application of polymeric composite connections*. Mottram JT and Turvey GJ (eds), European Commission, Brussels/Luxembourg, (1998), 15-26.
2. Turvey GJ. Bolted connections in PFRP structures. *Progress in Structural Engineering Materials* 2000;2(2): 146-56.
3. Turvey GJ. Bolted joints in pultruded glass fibre reinforced polymer (GFRP) composites. In *Composite joints and connections*. Camanho P and Tong L (eds), Cambridge, Woodhead Publishing Limited, (2011), 77-111.
4. Turvey GJ. Frame connections. In *Semi-rigid behaviour of civil engineering structural connections, COST C1: State-of-the-art review on design, testing, analysis and application of polymeric composite connections*. Mottram JT and Turvey GJ (eds), European Commission, Brussels/Luxembourg, (1998), 27-49.
5. Turvey GJ, Cooper C. Review of tests on bolted joints between pultruded GRP profiles. *Proceedings of the Institution of Civil Engineers: Structures and Buildings* 2004; 157(3):211-33.
6. Clarke JL, (ed). *Structural design of polymer composites: EUROCOMP design code and handbook*. London: E & FN Spon; 1996.
7. Mosallam AS. *Design guide for FRP composite connections*. ASCE manuals and reports on engineering practice no.102. Reston, VA: ASCE; 2011.
8. Anon. *Pre-Standard for load and resistance factor design (LRFD) of pultruded fiber reinforced polymer (FRP) structures*. Reston, VA: ASCE; 2010.
9. Keller T, and de Castro J. System ductility and redundancy of FRP beam structures with ductile adhesive joints. *Composites Part B: Engineering* 2005;36(8):586-96.
10. Turvey GJ. Effects of bonded splice joints on the flexural response of pultruded fibre reinforced polymer beams. *Applied Mechanics and Materials* 2010;24-25:401-6.
11. Turvey GJ. Flexure of pultruded glass-fibre-reinforced polymer beams with bonded splice joints. *Proceedings of the Institution of Civil Engineers: Structures and Buildings* 2011;164(SB4):333-44.
12. Nagaraj V. *Static and fatigue response of GFRP pultruded beams with and without connections [MSCE thesis]*. Morgantown, West Virginia, West Virginia University; 1994.
13. Nagaraj V, Gangarao HVS. Fatigue behaviour and connection efficiency of pultruded GFRP beams. *Journal of Composites for Construction* 1998;2(1):57-65.
14. Hai N, Mutsuyoshi H. Structural behaviour of double-lap joints of steel splice plates bolted/bonded to pultruded hybrid CFRP/GFRP laminates. *Construction and Building Materials* 2012;30:347-59.

15. ABAQUS 6.14 User Documentation, Internet Manual, Simulia, 2014. (<http://50.16.176.52/v6.14/index.html>)
16. Turvey GJ, Cerutti X. Flexural behaviour of pultruded glass fibre reinforced polymer composite beams with bolted splice joints. *Composite Structures* 2015;119:543-550.
17. Case J, Chilver Lord, Ross CTF. *Strength of material and structures*. Oxford: Butterworth Heinemann; 4th Edition Reprinted 2003.
18. Strongwell. *EXTREN® Fiberglass Structural Shapes: Design Manual*, Bristol, VA, USA;1989.

ACCEPTED MANUSCRIPT

List of Figures

- Figure 1:** Details of the symmetric halves of the pultruded GFRP splice plates: (a) outer plate and (b) inner plate [Dimensions in mm]
- Figure 2:** Side and end elevations of pultruded GFRP six-plate bolted splice joints: (a) 610 mm joint, (b) 410 mm joint, (c) 210 mm joint and (d) end elevations of all three joints [Not to scale and fillet radii not shown]
- Figure 3:** Details of four-point flexure test setup for pultruded GFRP simply supported beams with mid-span bolted splice joints
- Figure 4:** Mid-span cross-section of a six-plate splice joint showing the positions of the uniaxial strain gauges bonded on the outer surfaces of the splice plates [Not to scale and fillet radii not shown]
- Figure 5:** Image of a four-point flexure test on a pultruded GFRP simply supported beam with a mid-span bolted splice joint.
- Figure 6:** Repeatability of the load versus mid-span deflection for four-point flexure tests on simply supported pultruded GFRP beams with mid-span two- and six-plate bolted splice joints [Note: N = number of splice plates, T = bolt torque and Ls = 410 mm]
- Figure 7:** Repeatability of the load versus support rotation for four-point flexure tests on simply supported pultruded GFRP beams with mid-span two- and six-plate bolted splice joints [Note: N = number of splice plates, T = bolt torque and Ls = 410 mm]
- Figure 8:** Repeatability of the moment versus splice joint rotation for four-point flexure tests on simply supported pultruded GFRP beams with mid-span two- and six-plate bolted splice joints [Note: N = number of splice plates, T = bolt torque and Ls = 410 mm]
- Figure 9:** Transverse stiffness versus splice plate length of two-plate bolted splice joints for low and high bolt torques [Note: N = number of splice plates and T = bolt torque]
- Figure 10:** Transverse stiffness versus splice plate length - effects of bolt torque and number of splice plates
- Figure 11:** Percentage increase in transverse stiffness versus splice plate length – effects of: (i) increased bolt torque and (ii) increased bolt torque and number of splice plates [Relative to the transverse stiffness of a bolted splice joint with N = 2 and T = 3 Nm]
- Figure 12:** Percentage increase in rotational stiffness versus splice plate length for a two-plate splice joint – effect of increasing the bolt torque to 20 Nm from 3 Nm (Reference value)
- Figure 13:** Rotational stiffness versus splice plate length - effects of bolt torque and number of splice plates
- Figure 14:** Percentage increase in rotational stiffness versus splice plate length – effects of: (i) increased bolt torque and (ii) increased bolt torque and number of splice plates [Relative to the rotational stiffnesses of bolted splice joints with N = 2 and T = 3 Nm]
- Figure 15:** Six-plate bolted splice joint cross-sections: (a) original cross-section and (b) transformed cross-section [Not to scale and fillet radii and bolts not shown]
- Figure 16:** $\frac{M}{EI}$ - diagram for the half-span of the simply supported pultruded GFRP beam with a six-plate 610 mm long bolted splice joint at mid-span
- Figure 17:** Difference between the experimental and calculated support rotations applied as a rigid body rotation at support B to produce the mid-span deflection correction δ^a_c and the estimated slip

between the splice plates and the flanges over the beam's half-span (exaggerated scale drawing)

Table 1

Average elastic longitudinal tension moduli of pultruded GFRP beam and splice plate material

Profile Type	Longitudinal Elastic Modulus [GPa]
Wide Flange Beam (152 x 152 x 6.4 mm)	20.57 17.2*
Flat Plate (6.4 mm thick)	18.1 12.4*

*Value given in the Strongwell Design Manual [18]

Table 2

Test matrix for four-point flexure tests on simply supported pultruded GFRP beams with bolted mid-span splice joints

Length of Splice Plates [mm]	Number of Plates in Splice Joint	Bolt Torque [Nm]	Number of Repeat Tests
210	2	3	3
		20	3
	6	3	3
		20	3
410	2	3	3
		20	3
	6	3	3
		20	3
610	2	3	3
		20	3
	6	3	3
		20	3

Table 3

Transverse stiffnesses of simply supported pultruded GFRP beams with bolted mid-span splice joints loaded in four-point flexure

Splice Joint Length [mm]	Number of Splice Plates	Bolt Torque [Nm]	Transverse Stiffness (Test 3 Data) [kN/mm]	Transverse Stiffness (Tests 1 – 3 Average Data) [kN/mm]
210	2	3	0.229	0.217
		20	0.284	0.272
	6	3	0.308	0.284
		20	0.362	0.356
410	2	3	0.319	0.308
		20	0.371	0.363
	6	3	0.386	0.371
		20	0.441	0.433
610	2	3	0.342	0.334
		20	0.437	0.425
	6	3	0.437	0.419
		20	0.505	0.505

Table 4

Splice joint rotational stiffnesses of simply supported pultruded GFRP beams with bolted mid-span splice joints loaded in four-point flexure

Splice Joint Length [mm]	Number of Splice Plates	Bolt Torque	Rotational Stiffness (Test 3 Data)	Rotational Secant Stiffness (Test 3 Data)
		[Nm]	[Nm/mrad]	[Nm/mrad]
210	2	3	0.125	0.131
		20	0.191	0.190
	6	3	0.246	0.250
		20	0.320	0.325
410	2	3	0.235	0.235
		20	0.334	0.328
	6	3	0.332	0.325
		20	0.473	0.465
610	2	3	0.224	0.227
		20	0.369	0.372
	6	3	0.371	0.379
		20	0.515	0.519

Table 5

Formulae for the second moment of area components of the transformed bolted-splice joint cross-section

WF Beam [I_s]	Outer Splice Plates [I_{wo}]	Inner Splice Plates [I_{wi}]	Bolts in Outer Splice Plates [I_{b1}]	Bolts in WF Beam's Flanges [I_{b2}]	Bolts in Inner Splice Plates [I_{b3}]
$\frac{wh^3 - (w-t)t^3}{12}$	$\frac{w_{so} \{ (h+2t)^3 - (h-t)^3 \}}{12}$	$\frac{w_{si} \{ (h-2t)^3 - (h-t)^3 \}}{6}$	$\frac{w_{b1} \{ (h+2t)^3 - (h-t)^3 \}}{6}$	$\frac{w_{b2} \{ h^3 - (h-t)^3 \}}{6}$	$\frac{w_{b1} \{ (h-2t)^3 - (h-t)^3 \}}{6}$

Note: $w_{so} = \frac{E_s}{E_b} w_o$, $w_{si} = \frac{E_s}{E_b} w_i$, $w_{b1} = \frac{(E_{st} - E_s)}{E_b} w_b$, $w_{b2} = \frac{(E_{st} - E_b)}{E_b} w_b$ where E_b , E_s and E_{st} are

the longitudinal elastic moduli of the WF beam, the splice plates and the steel bolts respectively. w_o , w_i and w_b are the widths of the outer splice plate, the inner splice plate and the equivalent transverse width of the bolt, respectively.

Table 6

Areas A_i of the $\frac{M}{EI}$ -diagram in Figure 16

A_1	A_2	A_3	A_4	A_5	A_6	A_7	A_8	A_9
$\frac{Wa^2}{4E_b I_b}$	$\frac{Wab}{2E_b I_b}$	$\frac{0.045Wa}{2E_b (I_s + I_{wo})}$	$\frac{0.01Wa}{2E_b (I_s + I_{wo} + I_{wi} + I_{bl})}$	$\frac{0.9Wa}{2E_b (I_s + I_{wo})}$	A_4	A_5	A_4	$\frac{0.05Wa}{2E_b (I_s + I_{wo})}$

Note: E_b is the longitudinal elastic modulus of the WF beam.

Table 7

Distances in metres of the centres of the areas A_i ($i = 1-9$) from the support B in Figure 16

G_1	G_2	G_3	G_4	G_5	G_6	G_7	G_8	G_9
$\frac{2a}{3}$	$a + \frac{b}{2}$	$\alpha + 0.0225$	$\alpha + 0.05$	$\alpha + 0.1$	$\alpha + 0.15$	$\alpha + 0.2$	$\alpha + 0.25$	$\alpha + 0.28$

Note: $\alpha = a + b$

Table 8
Comparison of experimental and predicted rotations at the simple support B

Splice Plate Length [mm]	Number of Splice Plates	Bolt Torque [Nm]	Total Load [kN]	$\theta_{av} = \frac{ \theta_A + \theta_B }{2}$	Predicted $ \theta_B $	$\frac{ \theta_B }{\theta_{av}}$
				(Test 3) [rad]	[rad]	[%]
210	2	3	3.32	0.01349	0.00633	46.7
		20	4.07	0.01383	0.00776	56.1
	6	3	4.31	0.01377	0.00810	58.8
		20	5.38	0.01483	0.01011	68.2
410	2	3	4.69	0.01414	0.00842	59.5
		20	5.44	0.01456	0.00978	67.2
	6	3	5.60	0.01479	0.00978	66.1
		20	6.49	0.01513	0.01133	74.9
610	2	3	5.07	0.01316	0.00856	65.0
		20	6.35	0.01379	0.01071	77.7
	6	3	6.33	0.01368	0.01019	74.5
		20	7.46	0.01403	0.01202	85.7

Table 9

Comparison of experimental and predicted (with/without slip correction) mid-span deflections of simply supported pultruded GFRP beams with mid-span bolted splice joints

Splice Plate Length [mm]	Number of Splice Plates	Bolt Torque	Total Load	Mid-Span Deflection (Theory – No Slip)	Mid-Span Deflection (Theory – With Slip)	Mid-Span Deflection (Test)	With Slip Deflection/ Test Deflection	Estimated Slip in Half Splice Joint [mm]
		[Nm]	[kN]	[mm]	[mm]	[mm]		[mm]
210	2	3	3.32	5.76	16.47	15.00	1.098	0.544
		20	4.07	7.06	16.14	15.00	1.076	0.461
	6	3	4.31	7.32	15.80	15.00	1.053	0.431
		20	5.38	9.13	16.18	15.00	1.079	0.358
410	2	3	4.69	7.47	16.01	15.00	1.067	0.434
		20	5.44	8.67	15.82	15.00	1.055	0.363
	6	3	5.60	8.54	16.03	15.00	1.069	0.381
		20	6.49	9.89	15.56	15.00	1.037	0.288
610	2	3	5.07	7.41	14.30	15.00	0.953	0.350
		20	6.35	9.28	13.88	15.00	0.925	0.234
	6	3	6.33	8.62	13.39	15.00	0.893	0.265
		20	7.46	10.17	13.17	15.00	0.878	0.153

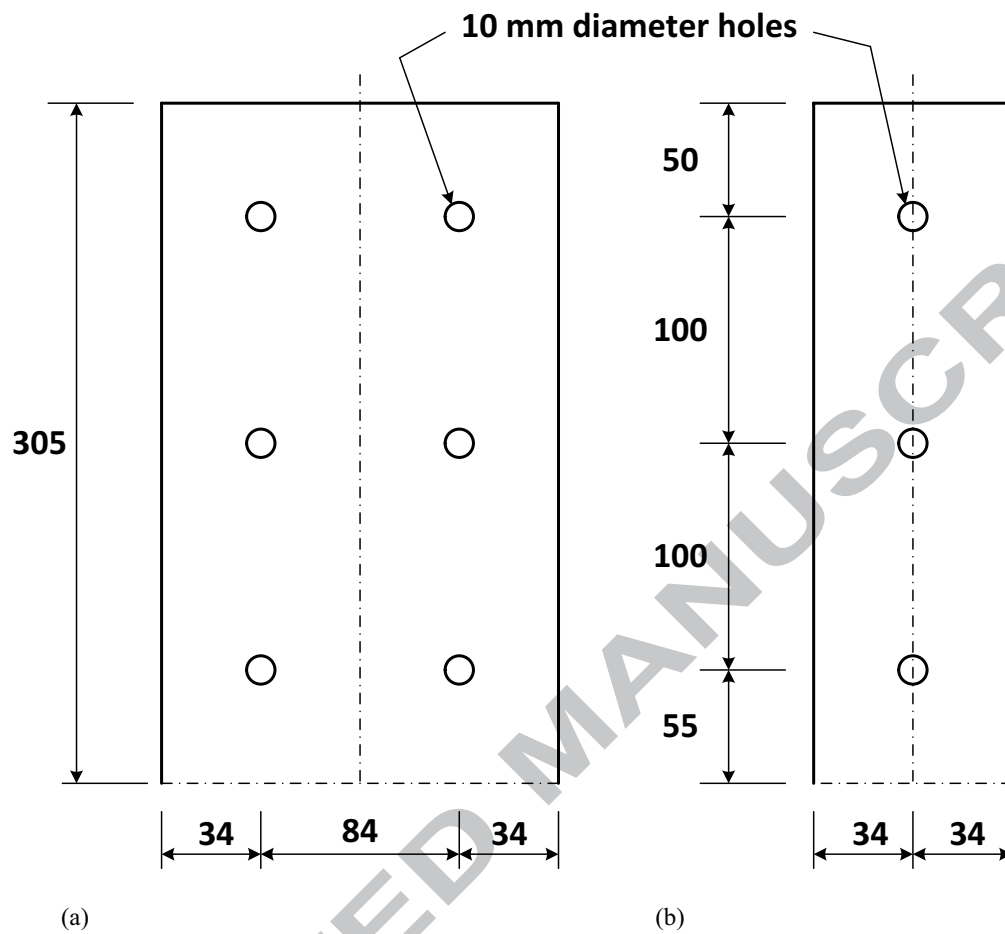


Figure 1

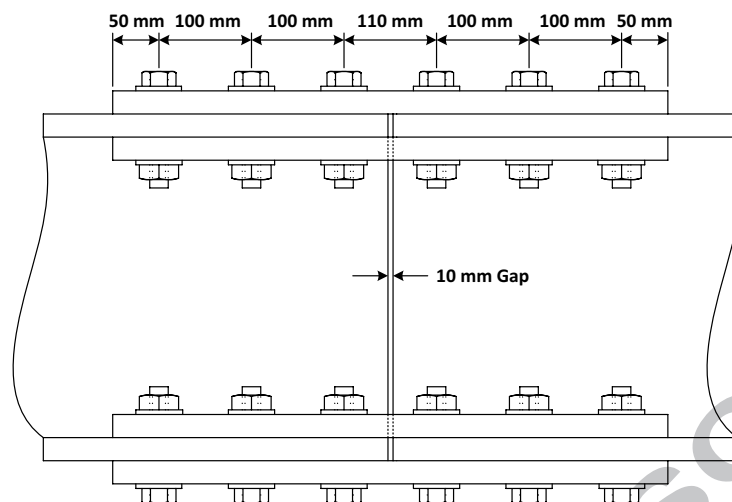


Figure 2(a)

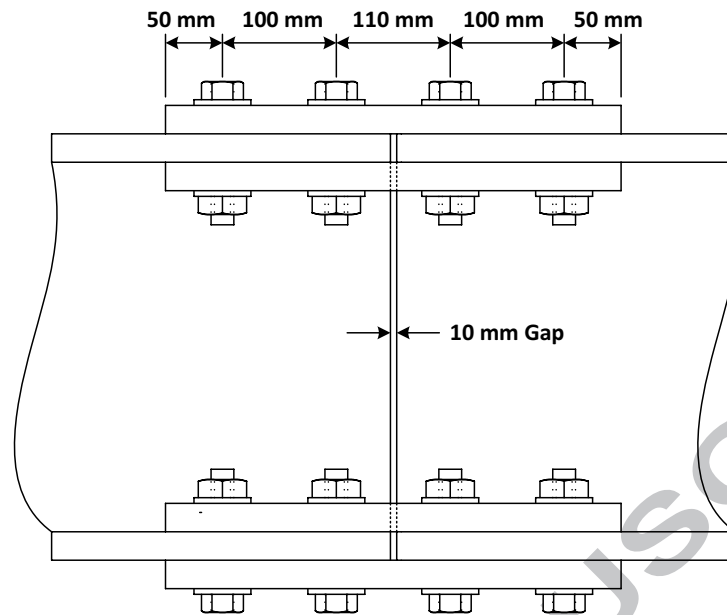


Figure 2(b)

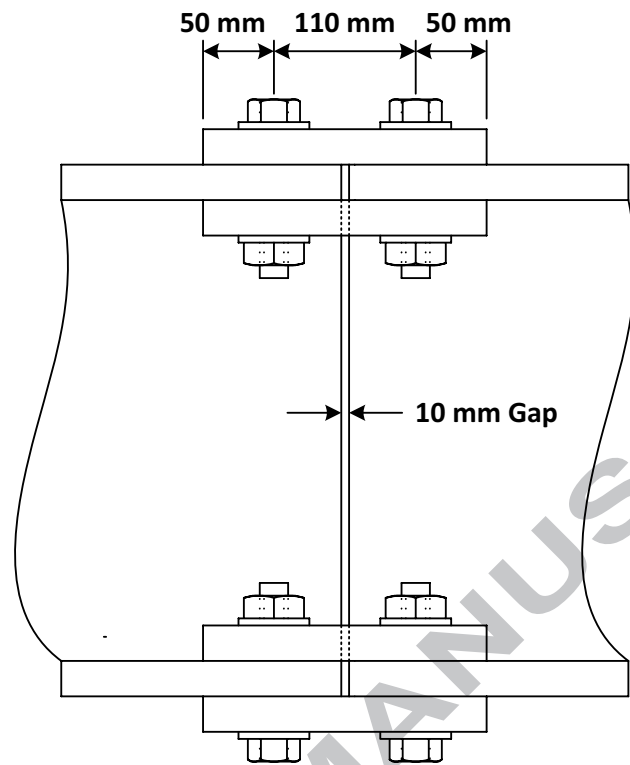


Figure 2(c)

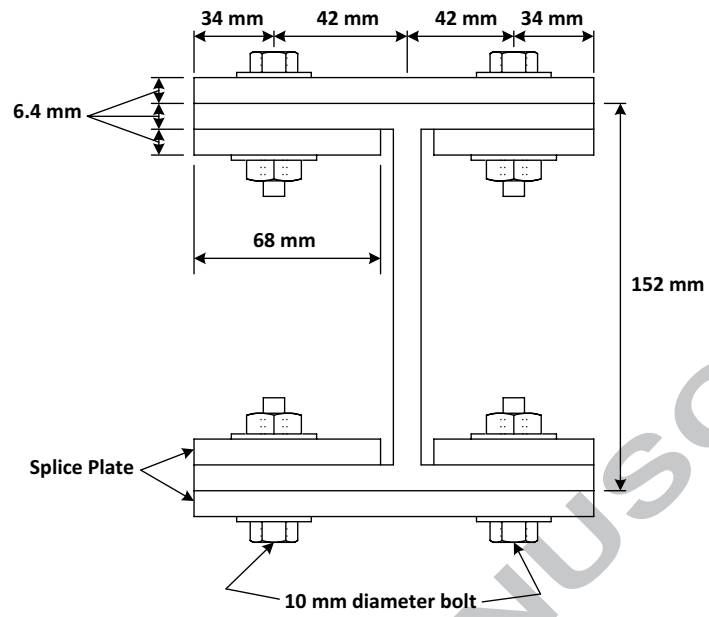


Figure 2(d)

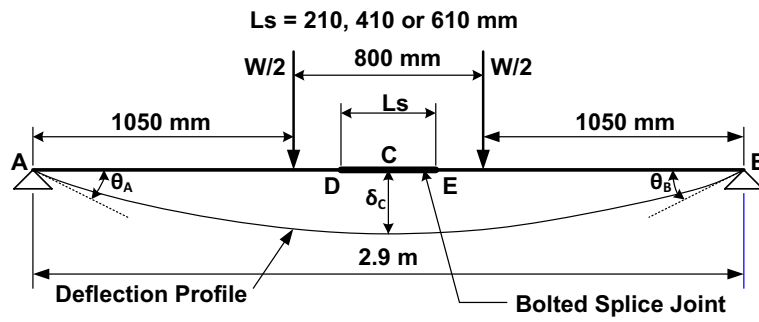


Figure 3

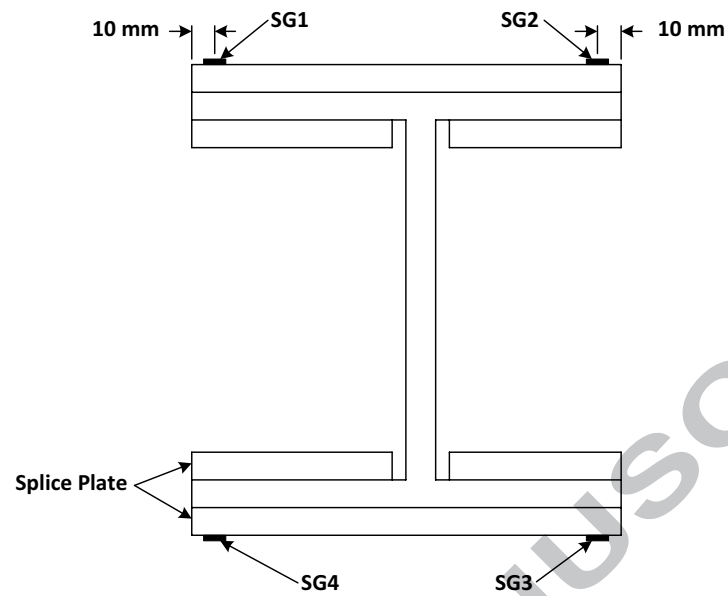


Figure 4

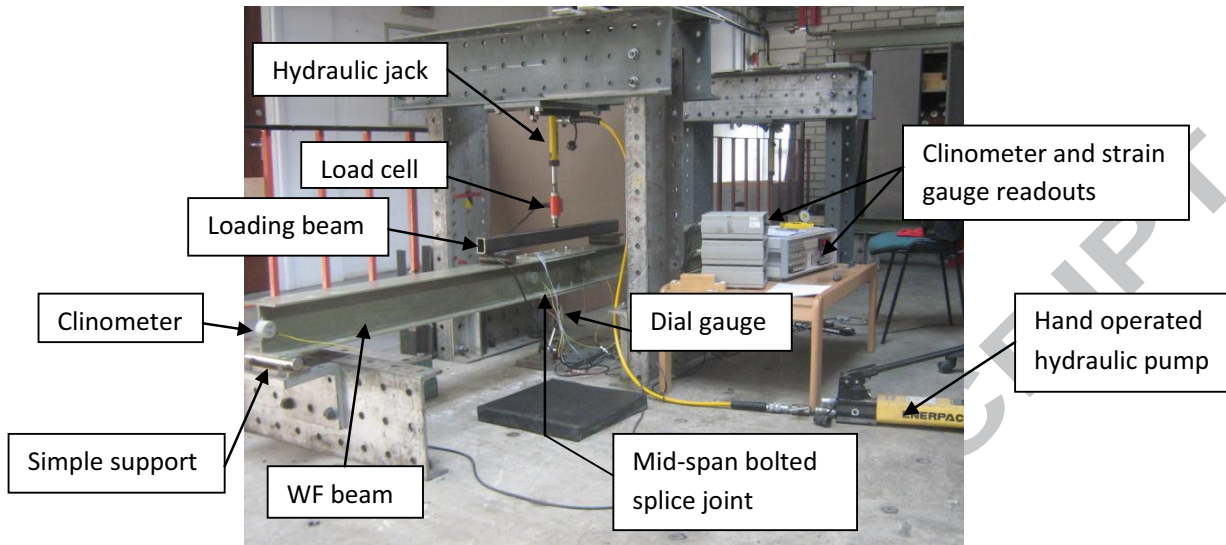


Figure 5



Figure 5 (jpg image without labels)
[Click here to download high resolution image](#)

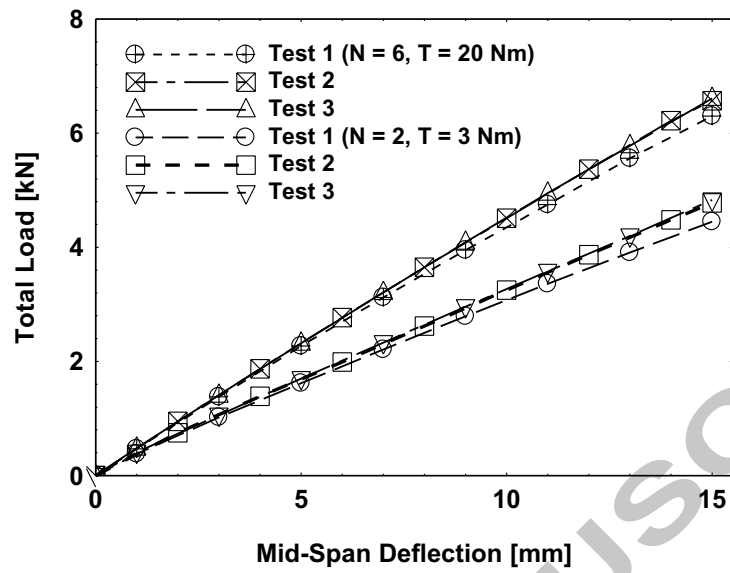


Figure 6

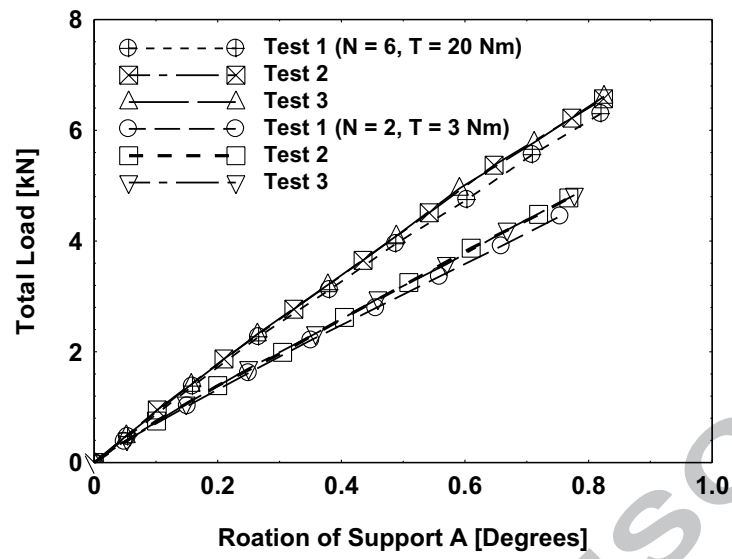


Figure 7

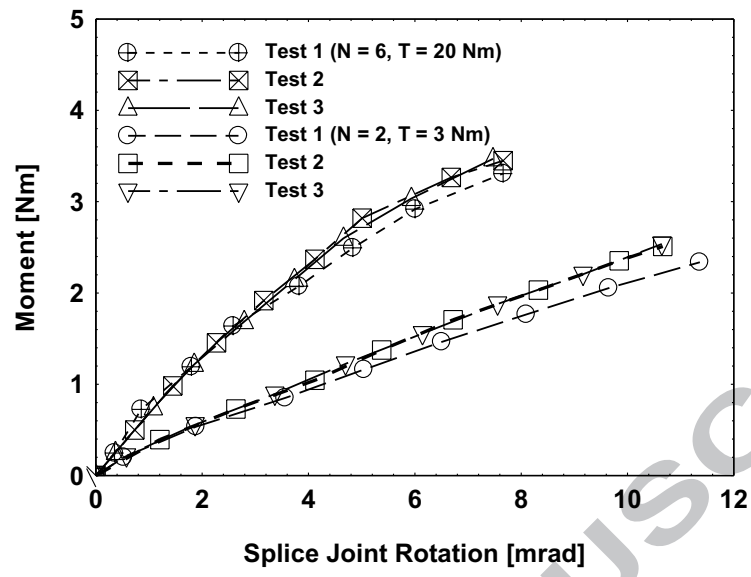


Figure 8

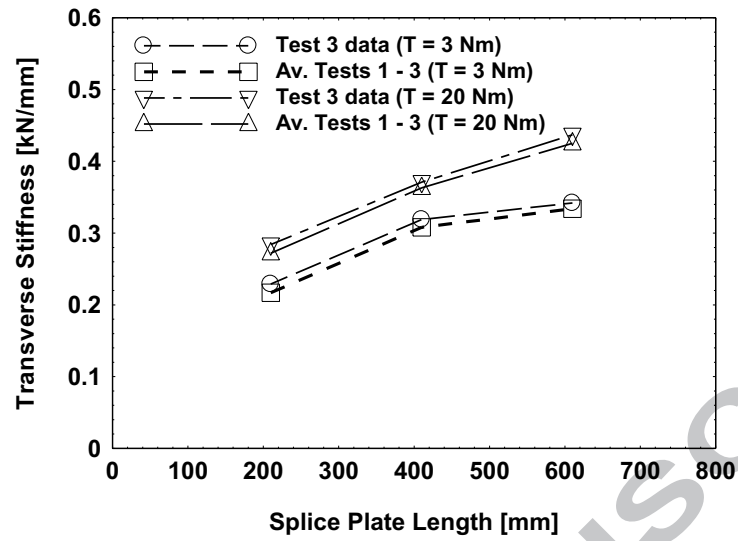


Figure 9

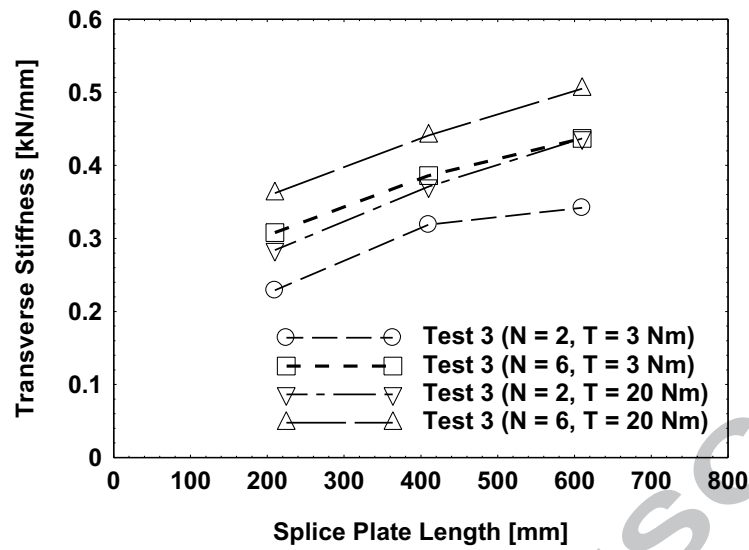


Figure 10

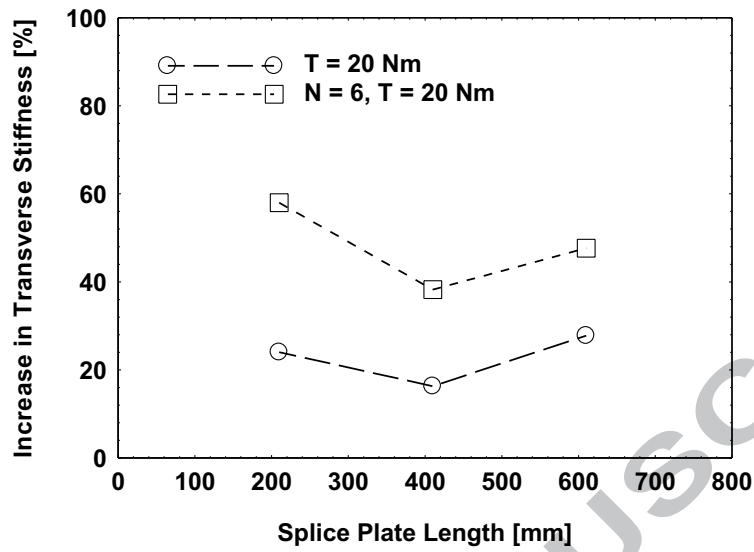


Figure 11

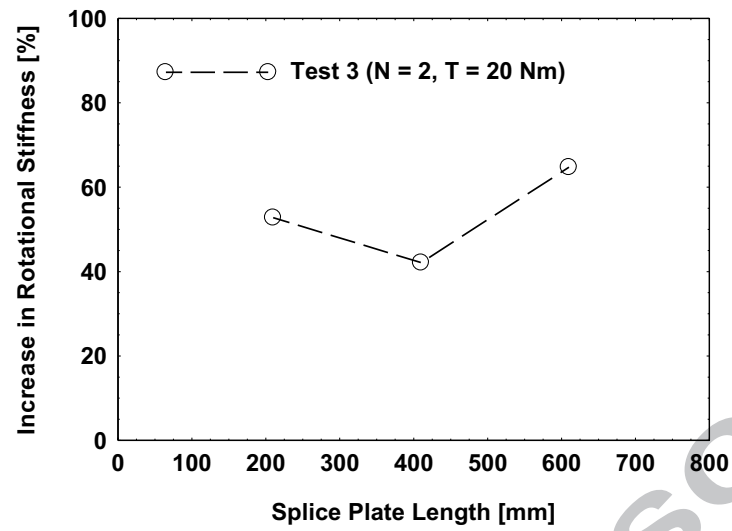


Figure 12

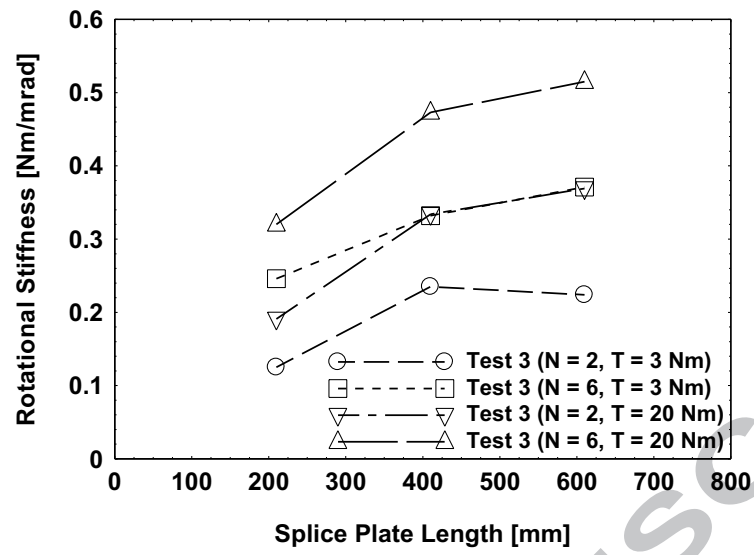


Figure 13

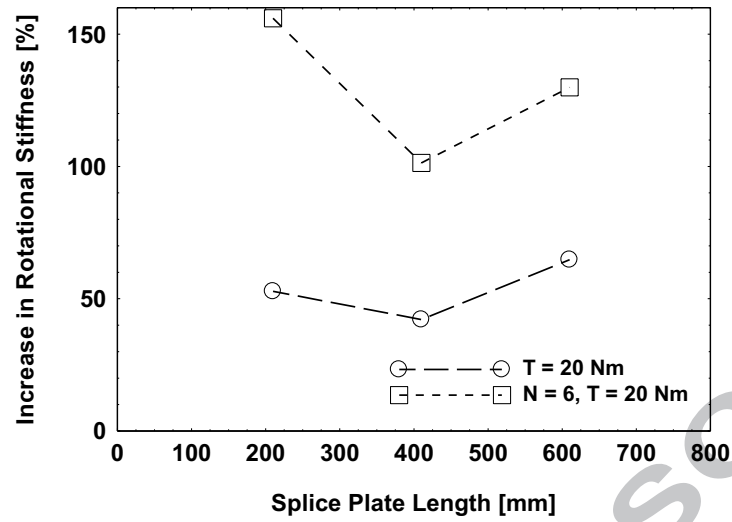


Figure 14

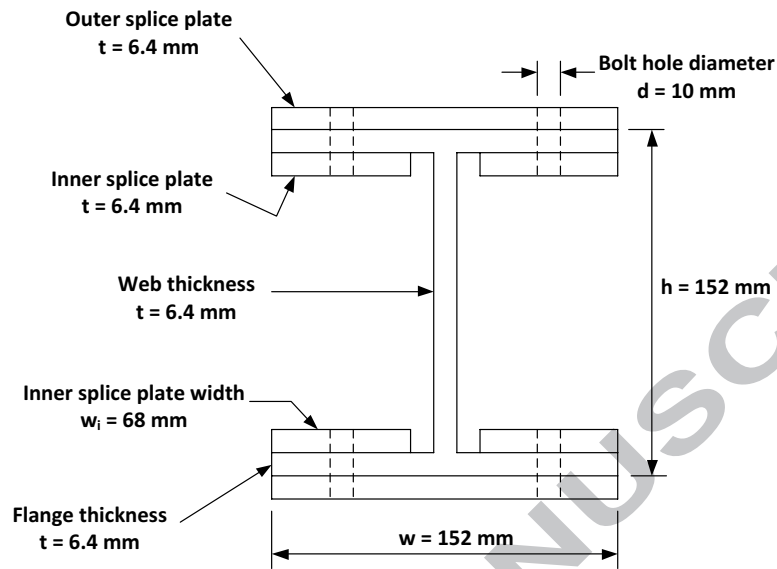


Figure 15(a)

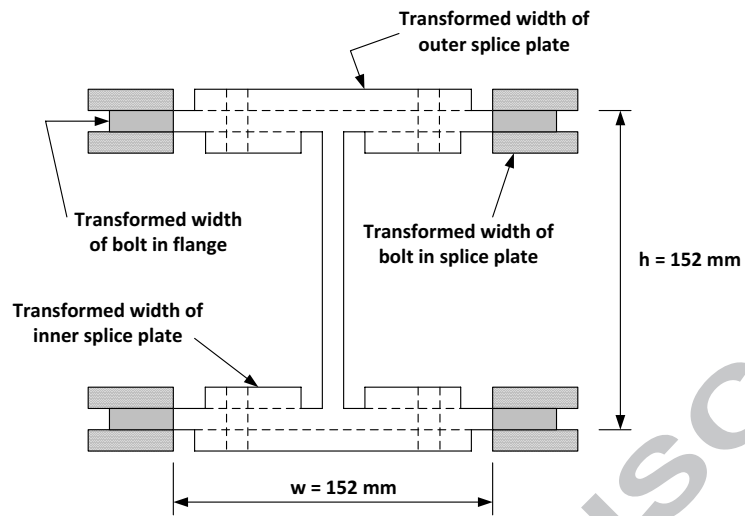


Figure 15(b)

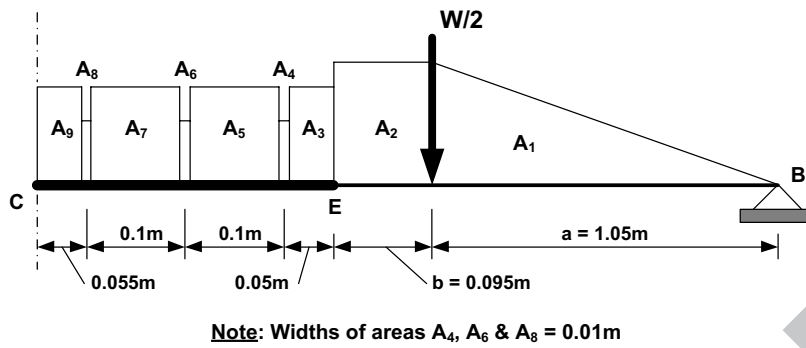


Figure 16

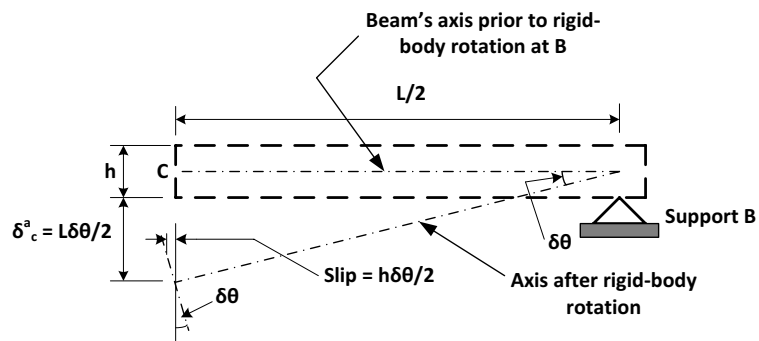


Figure 17

ACCEPTED MANUSCRIPT